ELSEVIER

Catalysis Today 52 (1999) 45–52

CATALYSIS TODAY

Synthesis and surface characterization of nanometric $La_{1-x}K_xMnO_{3+\delta}$ particles

Y. Ng Lee[1,a], Z. El-Fadli[2,b], F. Sapiña[b], E. Martinez-Tamayo[b], V. Cortés Corberán[a,*]

[a]*Instituto de Catálisis y Petroleoquímica, CSIC, Campus UAM Cantoblanco, 28049, Madrid, Spain*
[b]*Institut de Ciència dels Materials de la Universitat de València, Dr. Moliner 50, 46100, Burjassot (València), Spain*

Abstract

The use of a precursor-based synthetic method, namely, the freeze-drying of acetic acid solutions, allows the preparation of single-phased perovskites in the series $La_{1-x}K_xMnO_{3+\delta}$ ($x \leq 0.15$) at temperatures as low as 873 K. This soft treatment of the precursors yields products with high specific surface areas (20–26 $m^2\ g^{-1}$), constituted by uniform nanometric particles (30–50 nm), with their surface enriched in K and Mn. Samples prepared at 1073 K present lower specific surface areas (7–14 $m^2\ g^{-1}$), and show no K- and Mn-enrichment for $x \leq 0.15$. However, in samples with $x=0.20$ and 0.25, the presence of a secondary phase, $K_2Mn_4O_8$, is detected by X-ray diffraction, as well as a surface enrichment in K and Mn. These perovskite materials were found to be active for the catalytic combustion of ethane at low temperatures (573–648 K). As a general trend, the substitution of lanthanum by potassium decreases the areal rate, and for the more substituted samples ($x>0.10$), it increases the selectivity to ethene.

Keywords: $La_{1-x}K_xMnO_{3+\delta}$; Perovskites; X-ray diffraction; Acetate precursors; Freeze-drying; Ethane oxidation; Nanoparticles

1. Introduction

Cobalt and manganese lanthanide perovskites are active catalysts for the oxidation of hydrocarbons [1–10]. Among them, several partially substituted lanthanum compounds show a catalytic activity comparable to that of Pt/Al_2O_3 [3]. The performance of these catalysts depends on the surface composition, on their particle morphology, and in particular, on their specific surface area (SSA) [7,11]. This leads to the need of designing synthetic pathways alternative to the conventional ceramic method in order to obtain high purity, homogeneous powders with high SSA [12,13].

While systematic research has been carried out on alkaline-earth-doped lanthanide manganates, references to the preparation and the catalytic properties of alkali-metal-doped materials are scarce [13–19]. Voorhoeve et al. [13] studied the effect of substitution of alkali ions for La in $La_{1-x}K_xMnO_{3+\delta}$ (M=Na, K, Rb). They prepared several compositions by the ceramic method, which lead to very low surface areas (0.6–1.8 $m^2\ g^{-1}$). They reported that the substitution of La^{3+} by alkali ions in $LaMnO_3$ increases the catalytic activity for the reduction of NO. Johnson et al. [14] studied the preparation of substituted

*Corresponding author. E-mail: vcortes@icp.csic.es

[1]On leave from Universidad Central de Venezuela, Facultad de Ciencias, AP 47586, Los Charaguamos, Caracas 1041 A, Venezuela.

[2]On leave from the Departament de Chimie, Faculte des Sciences, Université Abdelmalek Essaadi, Tetouan, Maroc.

0920-5861/99/$ – see front matter
PII: S0920-5861(99)00061-9

$LaMnO_3$ perovskites to determine the effect of various A and B site substitutions on the catalytic activity for the oxidation of CO. They found that substitution of the cations Sr or K for La produced catalysts with the highest conversion rates. The authors used the freeze-drying or the spray-drying of nitrates and low calcination temperatures (973 K) as a method to obtain $La_{0.75}K_{0.25}MnO_3$ with high surface areas (17–18 $m^2\ g^{-1}$). More recently, France et al. [17] prepared alkali-doped $LaMnO_3$ by the ceramic method, and used it as catalysts for oxidative coupling of methane (OCM). They reported that, in comparison with the unsubstituted perovskite, the presence of alkali substitution increases both the conversion of methane and selectivity to C_2 hydrocarbons, although it decreases the surface area.

It should be noted that under most of the synthetic conditions reported (usually the ceramic method, with thermal treatments at temperatures higher than 1273 K), losses of potassium are systematically observed [18]. A similar effect has been observed in the preparation of other potassium-containing mixed oxides, such as potassium-doped $BaBiO_3$ superconducting materials [20], which indicates the difficulties in controlling cation stoichiometry by this synthetic method. Thus, besides the inherent advantages of the use of a precursor method [21], these alternative low temperature routes must play an essential role in the preparation of potassium-containing materials, avoiding the losses of potassium oxide at the high temperatures usually used in the ceramic method.

The aim of this work was the synthesis of high SSA potassium-doped lanthanum manganese perovskite series $La_{1-x}K_xMnO_{3+\delta}$ ($0 \leq x \leq 0.25$), formed by nanometric particles, by using a precursor-based synthetic method. The procedure consists of the thermal treatment of precursors obtained freeze-drying of acetic acid solutions containing the desired cations [22]. In the precursors, all the cations are randomly distributed at the atomic scale. This facilitates the incorporation of potassium into the perovskite lattice at the initial stage of the preparative procedure [22]. As the formation of the potassium-containing perovskite phase takes place at low temperatures, this avoids the evaporation of potassium, and a reliable stoichiometric control is achieved, in contrast with the ceramic method. The use of this method has allowed us to synthesize single-phased perovskites at low temperatures.

We report here the effect of the potassium substitution and of the calcination temperature on the physicochemical and catalytic properties of the perovskite particles. The particle size, morphology, SSA, surface metal ratios (calculated from XPS measurements) were measured. The oxidation of ethane was used as a catalytic test for characterizing the surface properties.

2. Experimental

Aqueous solutions of metal acetates with nominal atomic ratios La:K:Mn=$(1-x)$:x:1, with x=0.00, 0.05, 0.10, 0.15, 0.20 and 0.25, were prepared as follows. $KHCO_3$ was dissolved in 100 ml of glacial acetic acid. The addition of La_2O_3 led to a suspension, which was gently heated while stirring for 15 min. After addition of 20 ml of H_2O, a transparent solution was resulted. After cooling to room temperature, $Mn(CH_3COO)_2{\cdot}4H_2O$ was added and dissolved upon stirring. The mass of the different reagents was adjusted to give 5 g of perovskite. Droplets of the resulting pink pale acetic acid solutions were flash frozen by projection onto liquid nitrogen, and then, freeze-dried at a pressure of 10 Pa. In this way, dried solid precursors were obtained as pink loose powders.

In a series of experiments, various amounts of the pink powders were transferred to an alumina crucible, placed in a tubular furnace, and heated under dynamic oxygen atmosphere at 773, 873, 973, 1073 and 1173 K, respectively, for 12 h. This allowed us to determine the minimum temperature at which the perovskite phase is obtainable, that was 873 K (12 h) for all compositions investigated in this work.

Phase identification was carried out by powder X-ray diffraction (XRD) using a Siemens D500 computer-controlled diffractometer, with monochromatized Cu K_α radiation. Patterns were registered in steps of 0.08° in the 2θ angular range 20–65°, with integration times of 5 s per step. To reduce preferred orientation, the samples were dusted through a sieve onto the holder surface. The obtained patterns were compared with JCPDS data files.

Thermogravimetric analysis (TGA) was carried out with a Perkin-Elmer 7 system. The morphology

evolution was followed by scanning electron microscopy field emission (SEM) on a Hitachi 4100 instrument.

Physisorption measurements were performed with a Micromeritics ASAP 2000 instrument. The BET surface areas were determined by nitrogen adsorption at 77 K assuming a cross-section area of 0.162 nm^2 for the nitrogen molecule. Before the adsorption measurements, the samples were outgassed in vacuum at 423 K for 18 h.

X-ray photoelectron spectra (XPS) were recorded with a Fisons Scalab 200R spectrometer, using Mg K_α radiation (1253.6 eV) from an anode operated at 12 kV and 10 mA. The samples were pressed into small aluminum cylinders, mounted on a sample rod placed in a pretreatment chamber, and outgassed at 773 K for 1 h. The sample was then transferred to the analysis chamber. The pressure in the analyzer chamber was maintained below 6.66×10^{-7} Pa. The spectra were recorded in energy steps of 20 eV. The collection times were between 20 and 90 min, depending on the peak intensities. Binding energies (BE) were measured using the C 1s peak at 284.9 eV as internal standard (accuracy 0.1 eV). The intensities were estimated by calculating the integral of each peak after smoothing and subtraction of background, and fitting the experimental curves using a combination of Gaussian and Lorentzian profiles.

The oxygen non-stoichiometry, δ, was determined from the analysis of the temperature programmed reduction (TPR) profiles. These experiments were performed in a computer-controlled Micromeritics TPD/TPR 2900 apparatus. TPR profiles were obtained by passing a 10% H_2/Ar flow (50 cm^3 min^{-1}) through the sample. The amount of H_2 consumed was determined with a thermal conductivity detector (TCD). The heating rate was 10 K min^{-1}. Typical sample weight for these experiments was 50 mg.

The catalytic oxidation of ethane at 573–648 K was carried out at atmospheric pressure in a fixed bed reactor. Mixtures of ethane (4 mol%), oxygen (4–12 mol%) and helium (balance) were fed to the reactor with a residence time of 38 g h mol^{-1} C_2H_6, using the materials prepared at 873 K as catalysts. The catalyst load (0.36 g) was mixed with SiC bits (dilution 1:4 v/v) to reduce the heat release per unit volume. Perovskite powders were compacted and sieved to use the aggregates of size 0.25–0.42 mm in order to reduce the pressure drop along the catalytic bed. Reactants and products were analyzed by gas chromatography on a Varian 3400 instrument, equipped with a TCD, using Porapak QS (3 m) and molecular sieve 13X (1 m) columns. Under all reaction conditions, the mass and carbon balances were within 100±2%.

3. Results and discussion

3.1. Pyrolysis of the precursors

Thermal evolution of the precursors has been monitored by means of TGA and XRD. The TGA curve (not shown) corresponding to the thermal evolution in oxygen atmosphere (heating rate, 5 K min^{-1}; flow rate, 50 cm^3 min^{-1}) of the freeze-dried, precursor powders with x=0.15 shows two sharp weight losses at 338 and 493 K. The first one is associated with the evolution of acetic acid and/or water molecules retained in the precursor. The second weight loss can be associated with the thermal decomposition of the metal–acetate complex. Upon heating at higher temperatures, an additional small weight loss is observed (0.2%), which is associated with the decomposition of small quantities of carbonates and/or oxocarbonates formed during the decarboxylation process. No significant differences in TGA curves were observed by varying the K content.

Fig. 1 shows the XRD patterns of the products resulting from the thermal treatment of the freeze-dried powdered precursor, with x=0.15 at 873, 973, 1073 and 1173 K during 12 h under flow of oxygen. Their behavior is the representative of those observed for all the compositions. The most remarkable feature of these patterns is the observation, for all the compositions, of the perovskite as the only phase at a temperature as low as 873 K. Patterns of samples treated at 773 K show that the perovskite is already the major phase, but the presence of intense reflections associated with the intermediate phases indicates that the synthesis reaction is not complete. This result agrees well with those of Johnson et al. [14] who obtained a monophasic $La_{0.75}K_{0.25}MnO_3$ perovskite by calcining a freeze-dried nitrate precursor at 973 K. On the other hand, XRD patterns of samples with nominal composition x=0.20 and 0.25 at 1173 K show the presence of the secondary phase $K_2Mn_4O_8$

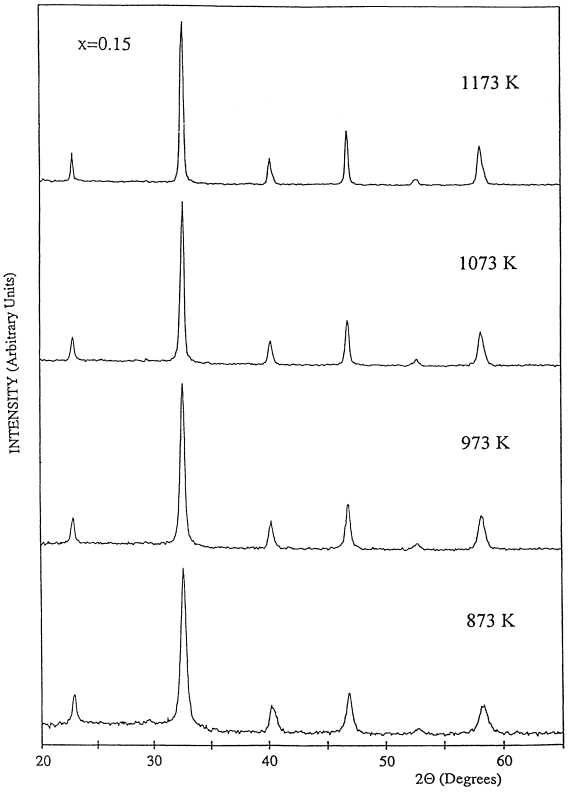

Fig. 1. XRD patterns of products resulting from the thermal treatment at 873, 973, 1073 and 1173 K of the freeze-dried precursor powder with x=0.15.

(JCPDS File 16-0205). However, no segregation was observed by SEM.

3.2. Microstructural characterization

Micrographs shown in Fig. 2 correspond to two representative samples. SEM images show that samples prepared at 873 K are constituted by uniform particles, having sizes between 30 and 50 nm. A progressive increase in the particle size is observed for samples prepared at higher temperatures. Thus at 1173 K, samples are constituted by homogeneous, well faceted particles of sizes between 80 and 140 nm.

The size of the crystallites can be calculated from XRD patterns by a standard Scherrer analysis of the half-width of the XRD peaks. Assuming rhombohedral symmetry for all the products (space group R-3c), the reflection at 46.7° is unique, and corresponds to the (0 2 4) indexation in the hexagonal setting. Well crystallized $Pb(NO_3)_2$ was used as standard to calibrate the intrinsic width associated to the equipment. Table 1 shows the crystallite sizes calculated for all the samples at the different calcination temperatures. As it can be observed, the results estimated from XRD are very similar for all the series. Crystallite size varies between 11 and 16 nm in samples calcinated at 873 K. At higher temperatures, crystallites grow and their sizes range between 31 and 38 nm at 1173 K.

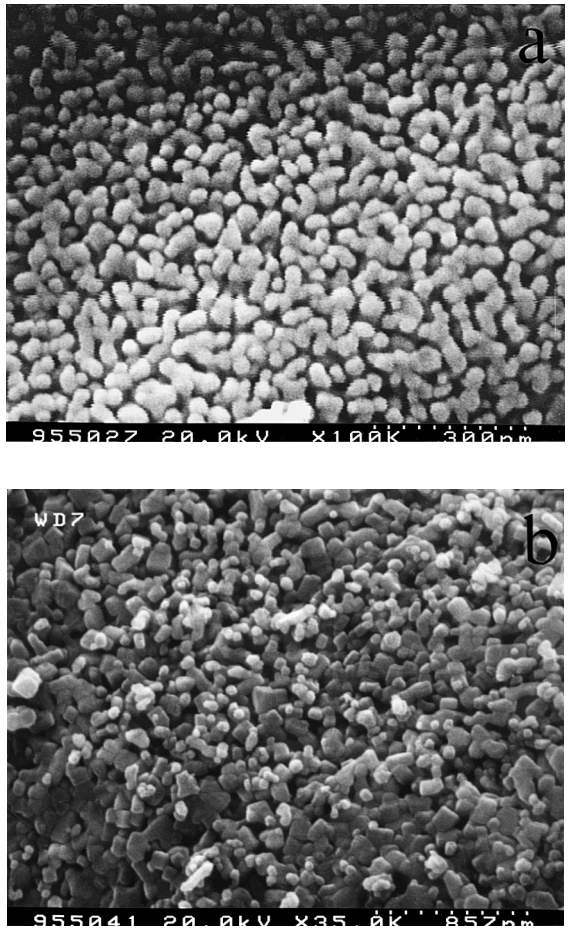

Fig. 2. SEM-FE micrographs of $La_{1-x}K_xMnO_{3+\delta}$ samples: (a) sample with x=0.05 prepared at 873 K and (b) sample with x=0.15 prepared at 1173 K.

3.3. Surface characterization

BET surface areas of the compounds are given in Table 2. With small variations among the different

Table 1
Crystallite size, $d_{0\,2\,4}$ (nm), calculated using the Scherrer's formula, of $La_{1-x}K_xMnO_{3+\delta}$ prepared at different calcination temperatures

Temperature (K)	x					
	0.00	0.05	0.10	0.15	0.20	0.25
873	11	13	16	16	15	16
973	13	18	19	21	21	21
1073	23	25	27	26	25	24
1173	36	38	37	33	31	35

compositions, the surface areas range from 20 to 26 $m^2\,g^{-1}$ for samples calcined at 873 K to 2–6 $m^2\,g^{-1}$ when calcined at 1173 K. The tendencies observed are those expectable according to the variation of crystallite size with the calcination temperature discussed above: the specific surface area decreases with increasing calcination temperature, regardless of the composition. The values of SSA obtained at 873 K are practically 10 times higher than those previously reported in the literature for $La_{1-x}K_xMnO_{3+\delta}$ perovskites compositions obtained by the ceramic method: 0.6–2.5 $m^2\,g^{-1}$ for $0.05 \leq x \leq 0.4$ [13], or 1.9 $m^2\,g^{-1}$ for $x=0.1$ [17]; and slightly higher than those reported for $x=0.25$ when prepared by freeze-drying or spray-drying of a nitrate precursor at 973 K (17–18.7 $m^2\,g^{-1}$) [14].

XPS measurements were performed on samples prepared at 873 and 1073 K. The results show that the binding energy (BE) of the La $3d_{5/2}$ peak was 834.8 eV, attributed to La^{3+}. The peak of Mn $2p_{3/2}$ shows two components, one centered at 641.2 eV (associated to Mn^{3+}), and other at 642.1 eV (associated to Mn^{4+}) [23]. The O 1s peak is complex, composed of one oxoanion component, at 530 eV, and two higher BE components, one around 531.6 eV, associated to hydroxyl oxygens (from adsorbed water), and the other around 532.4 eV, associated to carbonates [24]. The BE of the K 2p peak was 293.3 eV, attributed to K^+. The presence of carbonates in samples prepared at 873 K is corroborated by the observation of the O 1s peak at 532.4 eV, and the presence of the C 1s peak at 289.2 eV, characteristic of carbonates. Both features are absent in the spectra of samples prepared at 1073 K. These findings allow to confirm that the high temperature weight loss observed by TGA is due to the decomposition of surface carbonates and/or oxocarbonates.

The surface cationic compositions derived from the XPS data are presented in Fig. 3 as a function of the degree of substitution, x. Samples calcinated at 873 K show surface atomic ratios K/Mn and Mn/La systematically higher than the nominal composition of the samples. Chemical analysis by atomic absorption of samples prepared at 1273 K has shown that the actual content of potassium is practically equal to the nominal one in samples with $x \leq 0.15$, whereas small losses of potassium are observed for $x \geq 0.20$ samples [22]. This allows to assume that the bulk potassium content in samples with $x \leq 0.15$ calcined at lower temperatures is equal to the nominal one. Therefore, XPS results indicate a surface enrichment in potassium and manganese in all samples calcined at 873 K. At a variance, surface cationic ratios in samples with $x \leq 0.15$ prepared at 1073 K are very close to the nominal values. Thus, the increase of temperature allowed the homogenization of the cationic distribu-

Table 2
Specific surface areas ($m^2\,g^{-1}$) of $La_{1-x}K_xMnO_{3+\delta}$ prepared at different calcination temperatures

Temperature (K)	x					
	0.00	0.05	0.10	0.15	0.20	0.25
873	20	24	26	24	22	21
973	16	20	15	18	12	13
1073	13	14	10	9	8	7
1173	2	2	3	6	4	5

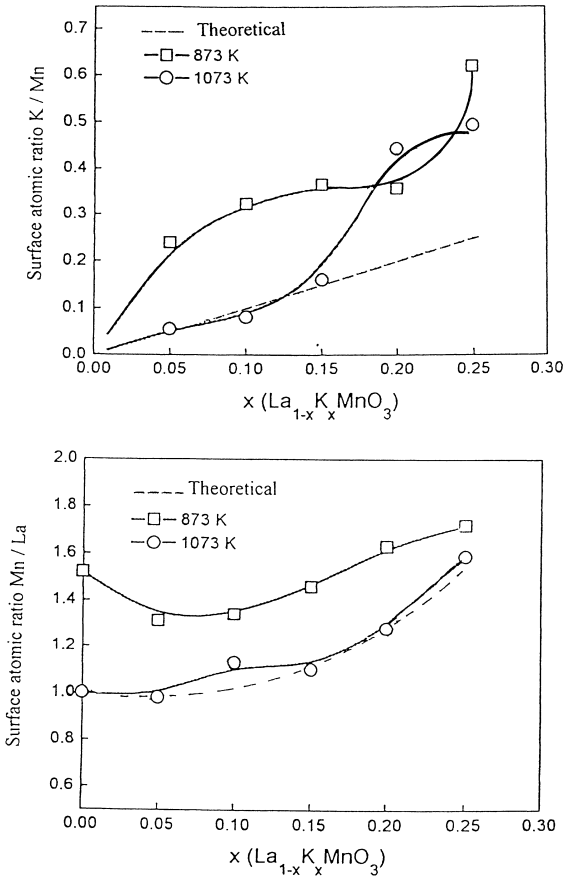

Fig. 3. XPS surface atomic ratios K/Mn (up) and Mn/La (down) in $La_{1-x}K_xMnO_{3+\delta}$ samples, prepared at 873 K (squares) and 1073 K (circles) as a function of the degree of substitution, x. Dashed lines correspond to nominal atomic ratios.

tion in the grains. Only samples with $x \geq 0.20$ prepared at 1073 K present a surface enrichment in K, but in this case it may be attributed to the presence of the secondary phase $K_2Mn_4O_8$, detected by XRD.

Table 3 shows the oxygen non-stoichiometry, δ, of samples with $x \leq 0.15$ prepared at 873 K, determined from their TPR profiles (not shown). The Mn^{4+} content is 26±4%, in good agreement with Voorhoeve et al. [13] who reported 30% Mn^{4+} for $LaMnO_{3.15}$ (x=0), and δ decreases with the substitution degree. Neutron diffraction studies of $LaMnO_{3.15}$ are consistent with a compact packing of oxygen ions with cationic vacancies at both La and Mn positions [25]. Thus, the substitution of lanthanum by potassium reduces the number of cationic vacancies and the

Table 3
Oxygen non-stoichiometry, δ, and Mn^{4+} contents in $La_{1-x}K_xMnO_{3+\delta}$ samples prepared at 873 K, calculated from TPR experiments

x	δ	Atom% Mn^{4+}
0.00	0.15	30
0.05	0.06	22
0.10	0.05	30
0.15	−0.04	22

negative value of δ indicates the presence of oxygen vacancies in the case of x=0.15 sample. Mn^{4+} contents determined by XPS increases with increasing x, varying from 41% for x=0 to 63% for x=0.25. These values are higher than the bulk Mn^{4+} contents determined by TPR (Table 3), indicating a preferential location of Mn^{4+} ions near the surface, where an enrichment in potassium is also found.

3.4. Catalytic properties

Under the used experimental conditions all the catalysts were active for the combustion of ethane, producing conversions from 1% to 5% at 573 K up to 40% at 648 K. The detected products were CO_2, H_2O and small amounts of ethane, which is consistent with a triangular reaction scheme involving the parallel formation of CO_2 and ethene and the consecutive combustion of ethane. In separate measurements of CO oxidation on these catalysts using a much lower residence time, CO was transformed completely into CO_2 at temperatures as low as 573 K. This would explain the absence of CO among the reaction products of ethane oxidation, carried out here at higher temperatures.

As a general trend, ethane conversion decreases with increasing of the degree of substitution, which is in contrast with the observed increase in activity caused by potassium substitution in NO reduction [13], CO oxidation [14] or OCM [17]. Fig. 4(a) shows the variation of areal rates of ethane oxidation over the $La_{1-x}K_xMnO_{3+\delta}$ catalysts with temperature. In all cases, ethane conversion increased with increasing temperature, but the areal rate (activity per surface unit) also decreased with the increase in potassium substitution. Within the experimental error, the calculated values of the apparent activation energy for

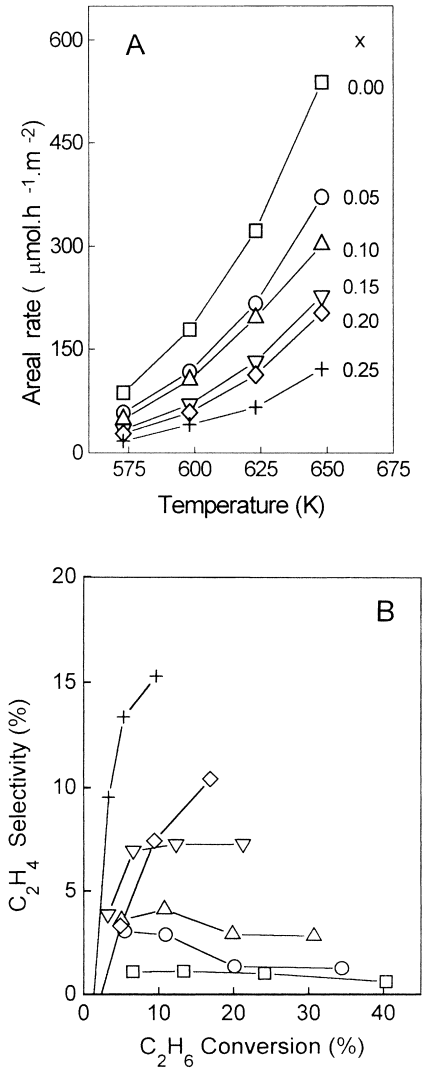

Fig. 4. (a) Areal rates of ethane oxidation on $La_{1-x}K_xMnO_{3+\delta}$ catalysts as a function of temperature and degree of substitution (x). (b) Variation of ethene selectivity with ethane conversion on $La_{1-x}K_xMnO_{3+\delta}$ catalysts. Feed composition: 4% C_2H_6, 12% O_2, He balance; W/F=38 g h mol^{-1} C_2H_6.

CO_2 formation were 18.4±0.2 kcal mol^{-1} for all the samples.

Potassium substitution also influences the evolution of ethene selectivity as a function of ethane conversion, as can be seen in Fig. 4(b). For samples with x=0.00 and 0.05, C_2H_4 selectivity remained constant, ca. 2%, in the whole temperature range. However, the catalysts with higher x presented an increase in the selectivity with the substitution degree and with the conversion. This indicates that the presence of potassium favors either the formation and/or the desorption of ethene formed via oxidehydrogenation of ethane. A parallel effect was observed by France et al. [17] in the OCM over $LaMnO_3$ and alkali-doped $LaMnO_3$: the presence of potassium increased considerably the selectivity to C_2 hydrocarbons formation. The authors found that the selectivity was correlated with higher binding energies for oxygen at the surface. It was shown that the existence of strongly bonded oxygen on the surface is effective to obtain more selectively hydrocarbons from methane, in contrast to the weakly adsorbed oxygen necessary for deep oxidation of hydrocarbons.

In a separate paper, we studied the influence of the oxygen partial pressure on ethane oxidation over potassium substituted perovskites [19]. It was concluded that the increase of K contents would decrease the ability of the perovskite to activate O_2 and to store active oxygen species, and would reduce the electrophilic character of these species. These two factors, that could be interpreted in terms of a higher oxygen binding energy, would explain the observed increase in the ethene selectivity with the increase of potassium contents.

4. Conclusions

The use of a precursor-based synthetic method, namely, the freeze-drying of acetic acid solutions, is a suitable preparation procedure to obtain perovskite materials with controlled potassium contents, avoiding the potassium loss inherent to the use of conventional ceramic methods. This method also allows to obtain high SSA single-phased potassium-doped lanthanum manganates $La_{1-x}K_xMnO_{3+\delta}$ at rather low temperature (873 K).

For $x \geq 0.15$, the materials obtained at high temperature (1073 K) were multiphasic, indicating the existence of an upper limit of solubility for potassium in this series. Below this limit, all the materials were monophasic, and the suitable choice of the calcination temperature may allow the control of the surface composition. At low temperatures, a surface enrichment of potassium and manganese can be achieved, while higher temperatures lead to an homogeneous cationic distribution.

In contrast with other catalytic reactions, the substitution of K for La decreased the intrinsic activity for ethane oxidation, but increased the selectivity to ethene. This effect could be due to a change of the mobility or the electrophilic character of the oxygen species at the surface, caused by the presence of potassium.

Acknowledgements

Financial support by the Spanish Comisión Interministerial de Investigación Científica y Técnica (CICYT) through projects MAT96-0688 and MAT96-1037 is gratefully acknowledged. Y. Ng Lee was supported by a grant from CDCH of UCV, Venezuela. Z. El-Fadli is grateful to the Spanish ''Instituto de Cooperación con el Mundo Arabe'' for a grant. The SCSIE of the Universitat de València is acknowledged for X-ray diffraction and SEM facilities.

References

[1] T. Nakamura, M. Misono, T. Uchijima, Y. Yoneda, Nippon Kagaku Kaishi (1980) 679.
[2] T. Seiyama, N. Yamazoe, K. Eguchi, Ind. Eng. Chem. Prod. Res. Dev. 24 (1985) 19.
[3] H. Arai, T. Yamada, K. Eguchi, T. Seiyama, Appl. Catal. 26 (1986) 265.
[4] T. Nitadori, T. Ichiki, M. Misono, Bull. Chem. Soc. Jpn. 61 (1988) 621.
[5] H.M. Zhang, Y. Shimizu, Y. Teraoka, N. Miura, N. Yamazoe, J. Catal. 121 (1990) 432.
[6] Z. Kaiji, L. Jian, B. Yingli, Catal. Lett. 1 (1988) 299.
[7] L.G. Tejuca, J.L.G. Fierro, J.M.D. Tascón, in: D.D. Eley, H. Pines, P.B. Weisz (Eds.), Advances in Catalysis, vol. 36, Academic Press, New York, 1989, p. 237.
[8] J.G. McCarty, H. Wise, Catal. Today 8 (1990) 213.
[9] B. de Collongue, E. Garbowsky, H. Primet, J. Chem. Soc., Faraday Trans. 87 (1991) 2493.
[10] C.B. Alcock, J.J. Carberry, Solid State Ionics 50 (1992) 197.
[11] R.J.H. Voorhoeve, D.W. Johnson, J.P. Remeika, P.K. Gallagher, Science 195 (1977) 4281.
[12] J. Kirchnerova, D. Klvana, J. Vaillancourt, J. Chaouki, Catal. Lett. 21 (1993) 77.
[13] R.J.H. Voorhoeve, J.P. Reeika, L.E. Trimble, A.S. Cooper, F.J. Disalvo, P.K. Gallagher, J. Solid State Chem. 14 (1975) 395.
[14] D.W. Johnson, P.K. Gallagher, F. Schrey, W.W. Rhodes, Am. Ceram. Soc. Bull. 55 (1976) 520.
[15] E.M. Vogel, D.W. Johnson, Thermochim. Acta 12 (1975) 49.
[16] E.M. Vogel, D.W. Johnson, P.K. Gallagher, J. Am. Ceram. Soc. 60 (1977) 31.
[17] J.E. France, A. Shamsi, M.Q. Ahsan, Energy Fuels 2 (1988) 235.
[18] T. Shimura, T. Hayashi, Y. Inaguma, M. Itoh, J. Solid State Chem. 124 (1996) 250.
[19] Y. Ng Lee, F. Sapiña, E. Martínez, J.V. Folgado, V. Cortés Corberán, Stud. Surf. Sci. Catal. 110 (1997) 747.
[20] G.V. Rama-Rao, U.V. Varadaraju, S.L. Mannan, Physica C 235–240 (1994) 761.
[21] A. González, E. Martínez Tamayo, A. Beltrán Porter, V. Cortés Corberán, Catal. Today 33 (1997) 361.
[22] Y. Ng-Lee, F. Sapiña, E. Martinez-Tamayo, J.V. Folgado, R. Ibañez, D. Beltrán, F. Lloret, A. Segura, J. Mater. Chem. 7 (1997) 1905.
[23] V. Di Castro, C. Furlani, M. Gargano, M. Rossi, Appl. Surf. Sci. 28 (1987) 220.
[24] K. Tabata, I. Matsumoto, D. Kohiki, J. Mater. Sci. 22 (1987) 1882.
[25] J.A.M. van Roosmalen, E.H.P. Cordfunke, R.B. Helmholdt, H.W. Zandbergen, J. Solid State Chem. 110 (1994) 100.